

## Adsorption of Pyrene at Model Hydrophobic Interfaces\*

Zlatica Kozarac<sup>a</sup>, Božena Čosović<sup>a</sup>, Dietmar Möbius<sup>b</sup>,  
and Wolfgang Budach<sup>b</sup>

<sup>a</sup>Ruder Bošković Institute, Center for Marine Research,  
P.O.B. 1016, 10001 Zagreb, Croatia

<sup>b</sup>Max - Planck - Institut für Biophysikalische Chemie, Postplac 2841,  
D-37018 Göttingen, Germany

Received February 27, 1996; accepted June 6, 1996

Adsorption behaviour of pyrene was studied at different model interfaces (air/water, air/lipid monolayer, mercury electrode/solution interface and lipid coated electrodes), with the aim to evaluate the most relevant processes influencing the distribution and effects of highly hydrophobic and slightly water soluble organic contaminants in natural aquatic systems. Studies have been performed by absorption, reflection and fluorescence spectroscopy, surface pressure and surface potential measurements and electrochemical methods. It was found that pyrene molecules incorporate into the hydrophobic core of lipid monolayers, thus influencing the charge and mass transfer through monolayers.

### INTRODUCTION

Pyrene and other polycyclic aromatic hydrocarbons (PAH-s) belong to the group of priority pollutants from the list of the Environmental Protection Agency<sup>1</sup> as some of the ubiquitous and highly dangerous organic pollutants entering natural aquatic systems due to the anthropogenic influence.

Although these compounds are poorly soluble in aqueous solutions, their accumulation at natural phase boundaries can be expected due to their

---

\* Dedicated to Marko Branica on the occasion of his 65<sup>th</sup> birthday.

highly hydrophobic nature.<sup>2</sup> Hydrophobicity of aromatic compounds increases with the number of benzene rings, from  $\log K_{o/w} = 2.13$  for benzene,  $\log K_{o/w} = 3.30$  for naphthalene and  $\log K_{o/w} = 4.45$  for anthracene<sup>3</sup> to  $\log K_{o/w} = 5.18$  for pyrene.<sup>4</sup>

As recently emphasized by Valsaraj,<sup>5</sup> experimental data on air-water interfacial adsorption of a large number of environmentally significant hydrophobic compounds, such as halogenated pesticides, polyhalogenated biphenyls, polycyclic aromatic hydrocarbons, *etc.* are still lacking.

Investigations of the equilibrium and kinetic parameters of relevant interfacial processes can be performed on real interfaces although model interfaces are very often more practical and convenient. We used two model interfaces, *viz.* the air/water and mercury electrode/solution interface. Although both interfaces are hydrophobic in their nature and show similar adsorption effects for many organic substances, especially aliphatic compounds, differences were observed in the case of aromatic compounds which were attributed to the  $\pi$ -electron interactions of the aromatic ring with mercury<sup>6</sup> resulting in stronger adsorption of the latter at the mercury/water interface than at the air/water interface. Our previously reported results<sup>7</sup> on adsorption behaviour of *para*-nitrophenol at air/water and mercury electrode/water interface are in good agreement with this scheme. Stronger adsorption of aromatic compounds at the mercury surface, as compared to their adsorption at the air/water interface, can be due to the preferably flat orientation of the molecules at the mercury surface. However, Gerovich<sup>8,9</sup> showed that the adsorbability of aromatic compounds at the mercury solution interface increases with the increasing number of benzene rings in the organic molecule, suggesting that the increased adsorption is due to the structural characteristics of the benzene ring.

Monolayer techniques used for the study at the air/water interface provide methods for organizing appropriate molecules in a planned way and studying interactions at the interface under controlled conditions.<sup>10</sup> They also enable transferring of the film from the air/water interface to the mercury surface.<sup>11-13</sup> Lipid coated electrodes have interesting practical applications. Interactions of the lipids with various species in the bulk solution can be monitored electrochemically, and ion and charge transfer across the film, as well as the interactions in the film, can be detected. Lipid coated electrode also represents a very sophisticated system for the study of the structure and functioning of biological membranes.

This paper reports on adsorption studies of pyrene at two model hydrophobic interfaces, namely at an air/solution interface and a mercury electrode/solution interface. Investigations have been performed by monolayer studies, spectroscopic techniques (absorption, reflection and fluorescence spectroscopy) and electrochemical methods.

## EXPERIMENTAL

### *Monolayer Studies at Air/Water Interface*

Surface pressure and surface potential were measured in a rectangular Teflon trough of inner dimensions  $56 \times 18 \text{ cm}^2$  and 1 cm deep, which was enclosed in a tight box and thermostated. A Wilhelmy balance (20 mm wide filter paper) was used to measure the surface pressure, and surface potential was measured using a vibrating plate condenser. Monolayers were compressed with a movable Teflon barrier of compression velocity between 0.06 and  $0.08 \text{ nm}^2/\text{min}/\text{molecule}$ .

Reflection spectroscopic measurements were performed using a reflection spectrometer for measurement under normal light incidence.<sup>14</sup> The reflection was measured and expressed as the difference  $\Delta R$  between the reflectivity from the surface covered with a monolayer and from the clean water surface. Reflection was measured at the maximum of the reflection spectrum, *i.e.* at 346 nm.

Fluorescence measurements were made by using a Perkin-Elmer Luminiscence spectrometer LS-5 with xenon lamp modified for *in situ* measurements at the air/water interface, in combination with a rectangular Teflon trough.<sup>15</sup> The monolayer was excited (using an optical fiber bundle) at an angle of  $37^\circ$  with respect to the air/water interface and the emission light was collected by a fiber bundle located perpendicularly above the illuminated monolayer (distance *ca.* 5 mm). The monolayers were excited at 350 nm and the emission was collected in the range from 350 to 550 nm. The spectra have been normalized with respect to the chromophore density.

### *Electrochemical Measurements*

Electrochemical studies were performed using the phase sensitive alternating current voltammetry.<sup>16</sup> The adsorption of pyrene from saturated solution onto the mercury surface was determined on the basis of capacitance measurements (out of phase signal) with prior accumulation at the potential of  $-0.4 \text{ V vs. Ag/AgCl}$  during 15, 30, 60, 120 and 300 s. The influence of the adsorbed pyrene layer on the cathodic and anodic processes of cadmium was followed by measuring Faradaic current (in phase measurements) after accumulation at the potentials of  $-0.4$  and  $-0.8 \text{ V vs. Ag/AgCl}$  during 15, 30, 60, 120 and 300 s, respectively.

Lipid films were prepared by spreading from pentane solutions onto the electrolyte solution, and then transferred to the mercury surface by vertical dipping of the electrode. Afterwards, films were studied by a.c. voltammetry.

Measurements were performed with a Polarecorder E-506 (Metrohm, Switzerland). A standard polarographic Metrohm cell of  $100 \text{ cm}^3$ , equipped with a three electrode system was used. A hanging mercury drop electrode (HMDE, Metrohm, Switzerland) of surface area  $A = 0.022 \text{ cm}^2$  was used as the working electrode, Ag/AgCl was used as the reference electrode and a platinum wire as the auxiliary electrode.

Pure nitrogen was used for deaeration of the solutions. All measurements were made in  $0.55 \text{ mol dm}^{-3} \text{ NaCl}$  as the supporting electrolyte.

### *Chemicals*

Pyrene, *p.a.* grade was purchased from Fluka Chemie AG., Switzerland.

Dimyristoylphosphatidylcholine (DMPC) and dipalmitoylphosphatidylcholine (DPPC) were from Larodan Chemicals.

Egg lecithin was purchased from Sigma.

Diocetadecyldimethylammonium bromide (DOMA) was from Kodak, Rochester, USA.

Sodium pyrene-3-sulphonate (NaPyS) was obtained from Molecular Probes.

Sodium chloride from Kemika, Zagreb, used as supporting electrolyte in electrochemical experiments, was heated for several hours at 723 K to eliminate traces of organic matter. A saturated solution of NaCl was additionally purified with charcoal.

Chloroform (HPLC) from Baker Chemicals and *n*-pentane, *p.a.* grade, from Kemika, Zagreb, were used as spreading solvents.

Deionised water from a Milli-Q system (Millipore) was used for preparing the subphase and all solutions.

## RESULTS AND DISCUSSION

### *Air/Water Interface*

Surface pressure measurements of saturated water pyrene solutions at a constant area showed that pyrene does not accumulate on free water surfaces in a time period of two hours. Surface pressure increased only by 3.5 mN/m, indicating almost none, or better to say negligible adsorption.

Assuming that pyrene molecules would adsorb better on lipid monolayers due to hydrophobic interactions, we have studied their adsorption on monolayers of DOMA and DPPC by measuring reflection kinetics during two hours after spreading and compression to 30 mN/m. Surface pressure was monitored simultaneously. The monolayers were spread on a pyrene saturated water subphase. The results are presented in Figure 1. No visible adsorption to DOMA and to DPPC monolayers can be seen from reflection measurements. Since only the chromophores present at the interface contribute to the reflection signal without influence of chromophores from the solution, the lack of the reflection signal could be explained by the lack of pyrene adsorption to the lipid monolayers. However, some other aspects of this problem arise. Concentration of saturated solution of pyrene was very low, *i.e.*  $4 \times 10^{-7}$  mol/dm<sup>3</sup>, as calculated from the absorption values of absorption spectra. This value is in good agreement with literature data.<sup>17</sup> Pyrene solution was placed in a shallow trough (1 cm deep) and no mixing of the solution could have been performed. Due to high hydrophobicity of pyrene molecule, the adsorption of pyrene on hydrophobic interfaces, like air/solution and lipid monolayers/solution interfaces, can be expected. The main reason why we did not observe adsorption from the bulk solution must have been the extremely low concentration and slow kinetics. In a much longer period of measurements, adsorption of pyrene should be noticed at these model interfaces. In order to avoid long time measurements, we prepared mixed monolayers using cospreading techniques, *i.e.* by spreading the mixed

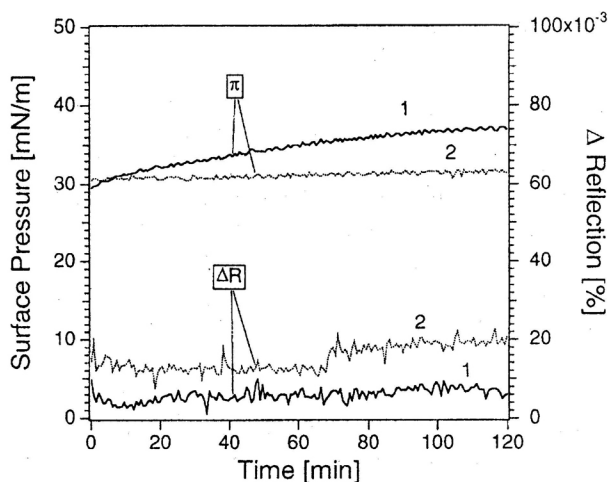


Figure 1. Surface pressure and reflection at 346 nm *versus* time of DOMA (curve 1) and DPPC (curve 2) monolayers spread on saturated solution of pyrene.

solutions of anchor lipid and pyrene on water surface. The surface pressure-molecular area ( $\pi$ - $A$ ) isotherms for DMPC monolayers and complex pyrene/DMPC monolayers, molar ratio 1:1, on pure water (pH = 5.6) are presented in Figure 2. DMPC spread on water (curve 1) exhibited the characteristics of liquid expanded film with phase transition at areas between 0.53 and 0.45 nm<sup>2</sup>. When pyrene is mixed with DMPC and spread on the water surface, expansion of mixed monolayer is observed in the whole area range compared to pure DMPC. Small phase transition disappeared, as well. Pyrene also influences charged monolayers of dioctadecyl-dimethyl-ammonium bromide and dioctadecyl malonic acid by expanding the area and affecting the phase transition of monolayers (data not presented here). However, the most significant effect was observed in mixed DMPC/pyrene monolayers.

Increase in molecular area is usually attributed to the penetration or incorporation of molecules into the monolayer. However, an expansion of the area can be observed even if adsorbed molecules are located underneath the monolayer, as shown recently in the studies of mixed monolayers of cyclic bisbipyridinium tetracations (BBP<sup>4+</sup>) and dimirystoylphosphatidic acid,<sup>18</sup> and sodium pyrene-3-sulphonate (NaPyS) and DOMA.<sup>19</sup> In both cases, BBP<sup>4+</sup> and PyS<sup>-</sup> were electrostatically bound to the polar head group of the lipid monolayer without being incorporated into the hydrophobic part.

However, interaction of pyrene with lipid monolayers can only be of hydrophobic nature. The expansion of the area in  $\pi$ - $A$  isotherms for the mixed pyrene DMPC monolayer, as well as the fact that the isotherm of mixed layer did not reach the isotherm of the pure DMPC monolayer at high film

pressures, shows clearly the incorporation of pyrene molecules into the DMPC monolayer.

Assuming hydrophobic interactions of pyrene with hydrophobic core of DMPC monolayers, we did not expect any change in surface potential. Values for surface potential  $\Delta V$  at 30 mN/m for DMPC; DMPC/pyrene, molar ratio 5:1; DMPC/pyrene, molar ratio 2:1 and DMPC/pyrene, molar ratio 1:1 are 450, 450, 420 and 420 mV, respectively, indicating that there is no electrostatic binding at the interface. In the case of electrostatically bound NaPyS to the monolayers of DOMA, the surface potential of DOMA is reduced from 995 to 810 mV for cospread monolayers of PyS<sup>-</sup>/DOMA, molar ratio 1:1.<sup>19</sup>

Fluorescence spectroscopy is very often used for the studies of interactions of unsubstituted and substituted pyrene with different lipid monolayers,<sup>20</sup> micelles<sup>21</sup> and vesicles.<sup>22</sup> Pyrene has a relatively long excited-state lifetime, high quantum yield of fluorescence, and the ability to form excimers. They are formed due to the ability of a ground state pyrene to diffuse to an excited state pyrene during the excited state lifetime.<sup>23</sup> The location of pyrene chromophores at the interface and association processes are affected by the hydrophobic moiety of the used lipids, subphase composition and type of substituents on pyrene chromophore. Our recent fluorescence spectroscopic measurements of complex DOMA/substituted pyrene (NaPyS) monolayers showed an excimer emission that was dependent on monolayer

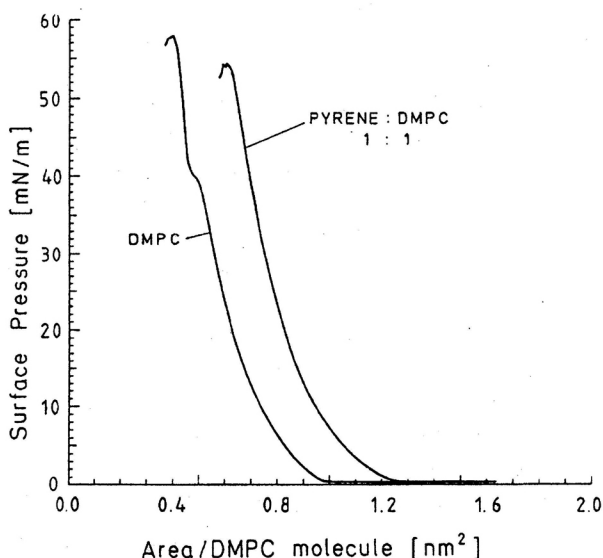


Figure 2. Surface pressure-molecular area ( $\pi$ -A) isotherms of DMPC monolayer and cospread pyrene/DMPC monolayer (molar ratio 1:1) on water.

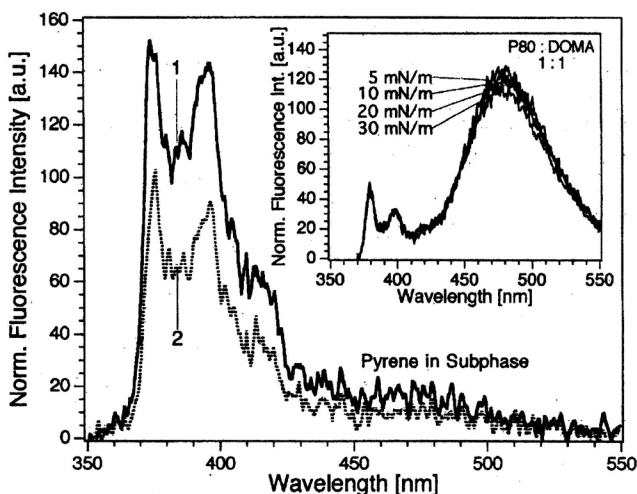


Figure 3. Fluorescence spectra of cospread pyrene/DOMA monolayers (molar ratio 1:1) at surface pressures of (1) 11 mN/m and (2) 26 mN/m on water.

The insert shows fluorescence spectra of cospread NaPyS/DOMA monolayers (molar ratio 1:1) at different surface pressures on water.

density, NaPyS concentration and subphase composition.<sup>19</sup> Surface pressure and surface potential measurements, as well as reflection spectroscopy, proved that pyrene chromophore was located under the head groups of lipid monolayer, which probably ensured close contact of pyrene chromophores, thus enabling excimer emission. In the case of incorporation of unsubstituted pyrene into the hydrophobic part of lipid monolayer, we can expect that pyrene molecules are not close enough to form excimers. We have measured the fluorescence spectra of cospread monolayers of DOMA, DPPC and DMPC with pyrene, and mainly observed monomer emission with a very small excimer emission. The main monomer bands are: for DOMA/pyrene monolayers at 375, 381 (weak), 392, 397 and 415 (weak) nm, for DPPC/pyrene monolayers at 375, 385 (weak) 395 and 418 nm, and for DMPC/pyrene at 376, 382 (weak) 390 and 395 nm. For all three monolayers, a very weak excimer emission was observed at 475 nm. The fluorescence spectra for complex DOMA/pyrene monolayer, in molar ratio 1:1, are presented in Figure 3. Fluorescence spectra for complex DOMA/NaPyS monolayer are given for comparison in the insert of Figure 3. The spectra are normalized with respect to the chromophore density. The difference between these systems is obvious. In the case of electrostatic interaction of  $\text{PyS}^-$  with positive charge on DOMA monolayer and location of pyrene under the monolayer, the conditions for pyrene excimer emission are fulfilled. If pyrene is placed into the lipid monolayer, the hydrophobic chains separate pyrene molecules and only

monomer emission can be observed in fluorescence spectroscopic measurements. The fluorescence spectra of cospread monolayers of DMPC and pyrene in molar ratio 1:1, are presented in Figure 4. The fluorescence intensity decreases at higher surface pressures, which can be caused by the self-quenching at high film pressures or by increasing dipol-dipol interactions in the monolayer due to the higher order of the fluorophores at higher film pressures. The fluorescence intensity at higher surface pressures could also decrease in the case of squeezing the pyrene molecules out from the monolayer but this should be also seen in the surface pressure – area isotherms. The same was observed for all three host molecules, namely for DOMA, DPPC and DMPC. Our data are in good agreement with the results reported by Wistus *et al.*,<sup>20</sup> about the incorporation of pyrene in the monolayers of eicosanoic acid. They also found only monomer emission. Since they used the host lipid in excess, they could not see excimer emission at all.

### Mercury Surface

Adsorption of organic molecules on the mercury electrode is a process of replacement of water dipoles by adsorbed organic hydrophobic or amphiphilic substances, resulting in the electrode double layer capacity change.<sup>24</sup> In a.c. voltammetry, the decrease in capacity or capacity current is a measure of adsorption. Adsorption is also a dynamic process and the structure of adsorbed layers changes with time and with the concentration of the solute.

In general, there is a distinct difference between aliphatic and aromatic compounds.<sup>25</sup> The adsorption of aliphatic compounds mainly depends on the chain length and the functional group, which determine the double-layer

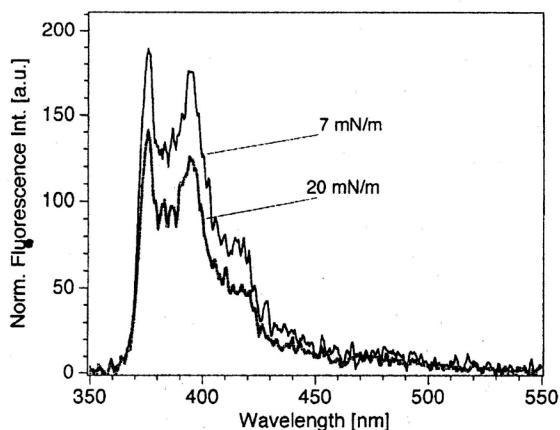


Figure 4. Fluorescence spectra of cospread pyrene/DMPC monolayers (molar ratio 1:1) at two different surface pressures at the air/water interface.



thickness and orientation. For aromatic substances, on the other hand, re-orientation processes become very important.<sup>26,27</sup> As shown for a number of aromatic compounds in these papers, three borderline cases for the orientation of molecules have to be distinguished: the two perpendicular orientations with the functional group either toward the metal or towards the solution, and flat orientation. For most substances, flat orientation dominates at low surface concentrations and positive potentials. It was also concluded that a very weak chemical bond and a small charge transfer between the metal and the aromatic molecule exist in the flat position, while for perpendicular orientation they are negligible.<sup>26,27</sup> In adsorption studies of polyaromatic hydrocarbons, problems arise from the fact that, due to their low solubility in water, higher concentrations can be obtained only in the presence of an organic solvent, as for example in alcoholic solutions.<sup>8,9</sup> Here we present adsorption data obtained in a saturated aqueous solution of pyrene containing  $4 \times 10^{-7}$  M pyrene. Capacity-potential curves obtained by phase sensitive a.c. voltammetry (out of phase measurements) for different adsorption times, namely 15, 30, 60, 120 and 300 sec, are presented in Figure 5. The capacity-potential curve of 0.5 M NaCl as basic electrolyte is denoted with the dashed line. The decrease in capacity, compared to the value for the basic electrolyte, is a measure of adsorption. The minimum capacity value  $C_{\min} = 14.3 \mu\text{F}/\text{cm}^2$  was determined for the adsorption of pyrene from saturated aqueous solution. This value is in good agreement with the reported values for flat orientation in adsorption of different aromatic compounds ( $10\text{--}15 \mu\text{F}/\text{cm}^2$ ).<sup>26,27</sup> The tensammetric peaks observed in the potential range between  $-1.2$  and  $-1.3$  V correspond to desorption processes of pyrene.

Regarding the adsorption of pyrene from aqueous solutions, it is important to stress that, at the concentration level of about  $80 \mu\text{g}/\text{l}$  pyrene, with prolonged adsorption time and stirring of the solution, surface coverages approach  $\theta \sim 1$ , as presented in Figure 6.

The capacitance measurements of  $5 \times 10^{-4}$  M pyrene in 0.5 M NaCl-2% (v/v) ethanol solution are illustrated in the insert of Figure 5. The minimum capacity value, determined as  $C_{\min} = 8.9 \mu\text{F}/\text{cm}^2$ , indicates a perpendicular orientation of pyrene at higher concentrations, similarly as reported for other aromatic compounds ( $5\text{--}8 \mu\text{F}/\text{cm}^2$ ).<sup>26,27</sup>

The structure and permeability of adsorbed layers was also tested using the redox process of Cd(II) as a probe. The adsorbed layer of organic molecules generally presents a barrier to the transport of ions and electrons at the interface, resulting in a decreasing electrode reaction rate.<sup>28,29</sup> Typical a.c. voltammetric waves, cathodic and anodic, of  $10^{-5}$  M  $\text{Cd}^{2+}$ , in the absence and presence of saturated solution of pyrene (accumulation time 300 s), are presented in Figures 7a and b. (curves 0 and 1). The dependence of the peak height of the cathodic and anodic a.c. voltammetric waves of  $10^{-5}$  mol  $\text{dm}^{-3}$  Cd on the adsorption of pyrene is also presented in Figure 6 (curves 2 and 3).

It can be seen that even a surface completely covered by an adsorbed layer of pyrene does not inhibit the electrode processes of cadmium ions.

Namely, quantitative interpretation of the adsorbed layer inhibition effect can be performed on the basis of the changes in the rate of the electrode processes of  $\text{Cd}^{2+}$ . The kinetic parameter, the apparent standard rate constant,  $k_s$ , of the electrode reduction of  $\text{Cd}^{2+}$  can be estimated from the shape and height of the a.c. or differential pulse voltammograms using theoretical curves obtained by digital simulation.<sup>29,30</sup> For a.c. voltammetry and the frequency of 75 Hz, used in this work, it can be estimated that the maximum peak current corresponds to the rate constant  $k_s \geq 1.7 \text{ cm/s}$ .<sup>31</sup> No change in the peak current in the presence of the adsorbed layer means that the rate constant does not fall below the above mentioned value for the method used.

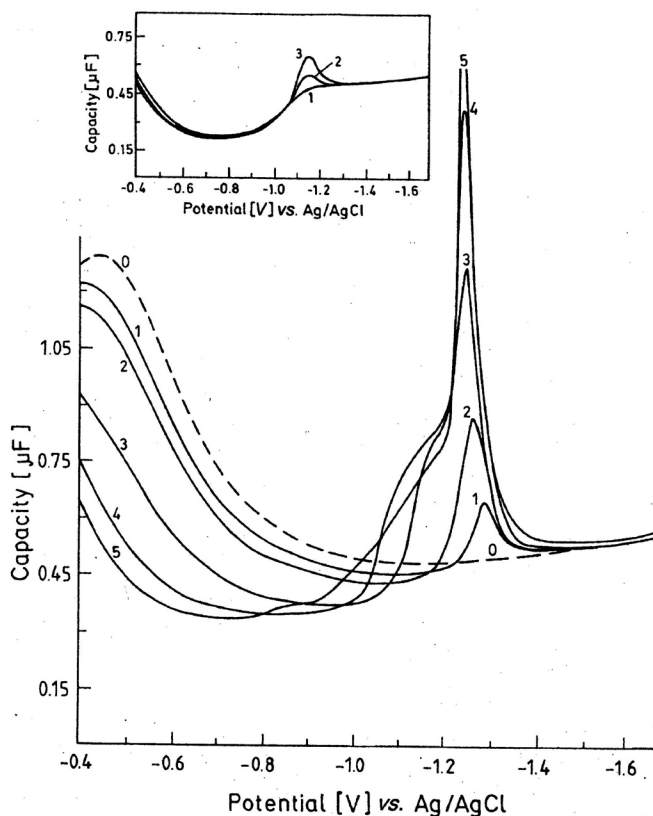


Figure 5. Capacity-potential curves for saturated aqueous solution of pyrene. Accumulation times: (1) 15, (2) 30, (3) 60, (4) 120 and (5) 300 s under stirring. Curve 0 denotes the capacity curve of  $0.5 \text{ mol dm}^{-3}$  NaCl.  $5 \times 10^{-4}$  M pyrene in  $0.5 \text{ M NaCl} - 2\% (v/v)$  ethanol solution. Accumulation times: (1) 0, (2) 60, (3) 300 s.

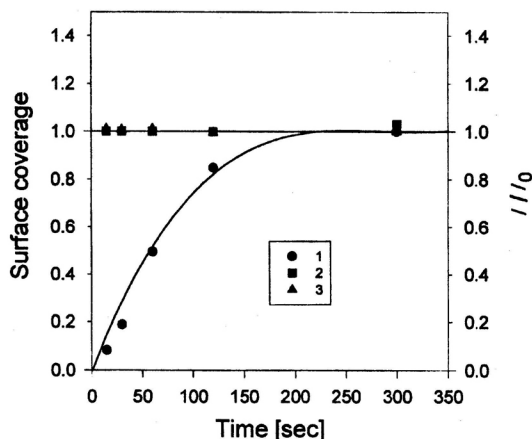


Figure 6. The apparent adsorption isotherm for saturated solution of pyrene. Accumulation at  $-0.4$  V under stirring (curve 1). Dependence of the relative height ( $I/I_0$ ) of the cathodic (curve 2) and anodic (curve 3) a.c. voltammetric waves of  $10^{-5}$  mol  $\text{dm}^{-3}$  Cd on the accumulation times. *Subphase*: saturated solution of pyrene in  $0.55$  mol  $\text{dm}^{-3}$  NaCl.  $I_0$  = anodic or cathodic wave height in the absence of pyrene. *Accumulation potential*:  $-0.4$  V (curve 2) and  $-0.8$  (curve 3).

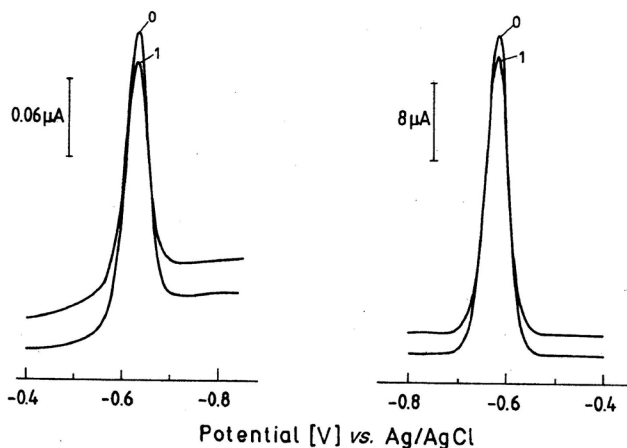


Figure 7. a) Cathodic a.c. voltammetric waves of  $10^{-5}$  mol  $\text{dm}^{-3}$   $\text{Cd}^{2+}$  in (0)  $0.55$  mol  $\text{dm}^{-3}$  NaCl and (1) saturated pyrene solution in  $0.55$  mol  $\text{dm}^{-3}$  NaCl. b) Anodic a.c. voltammetric waves of  $10^{-5}$  mol  $\text{dm}^{-3}$  Cd in (0)  $0.55$  mol  $\text{dm}^{-3}$  NaCl and (1) saturated pyrene solution in  $0.55$  mol  $\text{dm}^{-3}$  NaCl. *Accumulation time*: 300 s.

Inhibition effects on the cadmium reduction process have been studied with a number of adsorbable organic substances, representing either naturally occurring substances in the aquatic systems or different model substances.<sup>32</sup> We have observed in general that the adsorbed layers formed in neutral and alkaline solutions of natural biopolymers (proteins) and geopolymers (humic substances) do not inhibit the reduction of  $\text{Cd}^{2+}$  at the mercury electrode<sup>33</sup> but show a strong inhibition effect after acidification. There are two possible explanations for this; either (1) repulsive forces of the negatively charged functional groups of the polymer cause a formation of a more loose or porous adsorption layer in alkaline solution and a more condensed one after protonation in the acidic solution, or (2) the charge transfer process of cadmium can proceed *via* a bridging mechanism on negatively charged groups of the organic coating at the electrode surface. Taking into account that, for adsorption of aromatic molecules in the flat position, there is a weak chemical bond and a small charge transfer between the aromatic molecules and the mercury, we assume that a contact of  $\text{Cd}^{2+}$  with the adsorbed layer of pyrene through  $\pi$ -electrons of the layer enables the reduction process at the covered electrode surface.

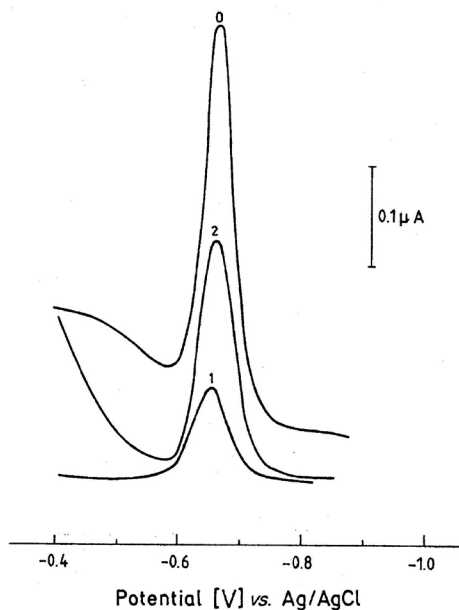


Figure 8. Cathodic a.c. voltammetric waves of  $10^{-5} \text{ mol dm}^{-3} \text{ Cd}^{2+}$ :

(0) in  $0.55 \text{ mol dm}^{-3} \text{ NaCl}$

(1) mixed monolayer of lecithin ( $0.614 \mu\text{g/cm}^2$ ) and pyrene ( $0.013 \mu\text{g/cm}^2$ )

(2) mixed monolayer of lecithin ( $0.0614 \mu\text{g/cm}^2$ ) and pyrene ( $0.13 \mu\text{g/cm}^2$ ).

It is known that electrode processes of cadmium are inhibited by phospholipid monolayers, which are formed by spreading from the organic solvent on the water surface, and then transferred to the mercury surface by vertical dipping of the electrode through the film.<sup>34,13</sup> The incorporation of pyrene into lipid monolayer was found by monolayer studies at the air/water interface in this work, as presented in Figure 2. This finding is also in good agreement with the published results of capacitance measurements at phospholipid-coated mercury electrodes in the presence of trace amounts of polynuclear aromatic hydrocarbons.<sup>35,36</sup> It can be also assumed that by incorporation of pyrene in the hydrophobic core of lipid monolayers, the structure of monolayers will change, thus influencing the transport of cadmium ions through the film. Our preliminary results for reduction of cadmium through monolayers prepared by cospreading technique of mixed solution of lecithin and pyrene in two different molar ratios, namely 10:1 and 1:10 are presented in Figure 8. If lecithin is mixed with pyrene, and then a complex monolayer is formed on the surface of electrolyte and transferred onto the mercury electrode, the reduction wave of cadmium increases due to the presence of pyrene in the film (curves 1 and 2).

More detailed study is needed which will include parallel capacitance measurements, monolayer studies and use of different electrochemical probes in order to get a better insight into the molecular structure of the adsorbed layers and their influence upon the mass and charge transfer across lipid monolayers.

#### *Relevance for Natural Phase Boundaries*

Natural aquatic systems contain a large number of organic substances with different functional groups and different hydrophobic properties. Surface active organic compounds which are released by phytoplankton, as products of their metabolism or compounds originating from decomposition and degradation processes of dead organisms, form the surface microlayer (50–100 m) which represents the interfacial region where many important bio-chemico-physical processes and flux of gases are taking place. Natural films are extremely complex, consisting of free fatty acids, alcohols, lipids, hydrocarbons and of more oxygenated molecules of higher molecular weights, such as the glycopeptido-lipid oligosaccharide complex. Transport of species like metals, organics and organisms does not occur only through the water column but is also very important at the air/water interface. The structure and composition of the surface microlayer can influence the geochemical cycles of many environmental pollutants.

In general, hydrophobic compounds are poorly soluble in water, so they are preferentially located at the air/water interface. Depending on whether they are volatile, partly volatile or non volatile, their transfer from the bulk

aqueous phase will be either to the vapour phase (volatization) or to the air/water interface (adsorption).<sup>2</sup> Most of the small hydrophobic compounds having large vapour pressures, tend to be in the vapour phase. In contrast, large hydrophobic molecules, having a low vapour pressure will remain at the air/water interface. Natural and anthropogenic hydrophobic compounds accumulate at the surface due to their hydrophobicity, incorporate in the »surface microlayer«, thus changing the structure of natural films.

The pyrene-lipid system was used in this work as a model for more general studies of the fate and transport of highly hydrophobic, poorly water soluble and environmentally significant compounds across the natural phase boundaries, and their influence on the processes of mass and energy transfer through them.

*Acknowledgments.* – We want to thank Werner Zeiss for technical assistance. This work was funded by the Croatian Ministry of Science. Financial support from the International Bureau of KFA, Jülich, within the bilateral agreement between Germany and the Republic of Croatia is gratefully acknowledged.

## REFERENCES

1. H. L. Keith and W. A. Telliard, *Environ. Sci. Technol.* **13** (1979) 416–423.
2. K. T. Valsaraj, *Chemosphere* **17** (1988) 875–887.
3. R. F. Rekker, *Elsevier Scientific Publishing Company*, 1977, pp. 83.
4. K. T. Valsaraj and L. J. Thibodeaux, *Separation Science and Technology* **25** (1990) 369–395.
5. K. T. Valsaraj, *Wat. Res.* **28** (1994) 819–830.
6. B. B. Damaskin, O. A. Petrii, V. V. Batrakov, *Adsorption of Organic Compounds on Electrodes*, Plenum Press, New York, 1971.
7. Z. Kozarac, B. Čosović, B. Gašparović, A. Dhathathreyan, and D. Möbius, *Langmuir* **7** (1991) 1076–1081.
8. M. A. Gerovich and O. G. Olman, *Zh. Fiz. Khim.* **28** (1954) 19–25.
9. M. A. Gerovich, *Doklady Akad. Nauk S.S.S.R.* **96** (1954) 543–546.
10. H. Kuhn and D. Möbius, In: *Investigations of surfaces and interfaces-Part B. Physical Methods of Chemistry Series*, B. W. Rossiter and R. C. Baetzold (Eds.), 2nd ed., Vol. IXB. John Wiley & Sons, Inc., 1993, pp. 375.
11. R. E. Pagano and I. R. Miller, *J. Colloid Interface Sci.* **45** (1973) 126–137.
12. A. Nelson and A. Benton, *J. Electroanal. Chem.*, **202** (1986) 253–270.
13. Z. Kozarac, R. Klarić, Đ. Dragčević and B. Čosović, *Colloids and Surfaces* **56** (1991) 279–291.
14. H. Grüniger, D. Möbius, and H. Meyer, *J. Chem. Phys.* **79** (1983) 3701–3710.
15. W. Budach, *Elektrostatische, dynamische und optische Eigenschaften von organisierten Monofilmen hinsichtlich des Aufbaus von Sensor-Schichtsystemen*, PhD Thesis, Göttingen, 1991, p. 16.
16. D. E. Smith, In: *Electroanalytical Chemistry*, A. J. Bard (Ed.), Vol. 1. Marcel Dekker, New York, 1966, pp. 1.
17. W. E. May, S. P. Wasik, and D. H. Freeman, *Anal. Chem.* **50** (1978) 997–1000.

18. R. C. Ahuja, P. L. Caruso, D. Möbius, G. Wildburg, H. Ringsdorf, D. Philp, J. A. Preece, and F. Stoddart, *Langmuir* **9** (1993) 1534–1544.
19. Z. Kozarac, R. C. Ahuja, and D. Möbius, *Langmuir* **11** (1995) 568–573.
20. E. Wistus, E. Mukhtar, M. Almgren, and S.-E. Lindquist, *Langmuir* **8** (1992) 1366–1371.
21. K. Tamori, Y. Watanabe, and K. Esumi, *Langmuir*, **8** (1992) 2344–2346.
22. G. P. LHeureux and M. Fragata, *J. Photochem. Photobiol. B: Biology* **3** (1989) 53–63.
23. von Th. Förster, *Angew. Chem.* **81** (1969) 364–374.
24. H. Jehring, *Elektrosorptionsanalyse mit der Wechselstrom- Polarographie*. Akademie-Verlag, Berlin, 1974, pp. 456.
25. E. Blomgren, J. O' M. Bockris, and C. Jesch, *J. Phys. Chem.* **65** (1961) 2000–2010.
26. D. Rolle and J. W. Schultze, *Electrochimica Acta* **31** (1986) 991–1000.
27. D. Rolle and J. W. Schultze, *J. Electroanal. Chem.* **229** (1987) 141–164.
28. J. Lipkowski and Z. Galus, *J. Electroanal. Chem.* **61** (1975) 11–32.
29. Z. Kozarac, S. Nikolić, I. Ružić, and B. Čosović, *J. Electroanal. Chem.* **137** (1982) 279–292.
30. N. Batina, Ph.D. Thesis, Univ. of Zagreb, 1986.
31. N. Batina and B. Čosović, *J. Electroanal. Chem.* **227** (1987) 129–146.
32. B. Čosović, In: *Aquatic Chemical Kinetics*; W. Stumm (Ed.), John Wiley, 1990, p. 291.
33. Z. Kozarac, B. Čosović, and V. Vojvodić, *Wat. Res.* **20** (1986) 295–300.
34. A. Nelson and H. van Leeuwen, *J. Electroanal. Chem.* **273** (1989) 183–199.
35. A. Nelson, *Anal. Chim. Acta* **194** (1987) 139–149.
36. A. Nelson, N. Auffret, and J. Readman, *Anal. Chim. Acta* **207** (1988) 47–57.

## SAŽETAK

### Adsorpcija pirena na hidrofobnim granicama faza

*Zlatica Kozarac, Božena Čosović, Dietmar Möbius i Wolfgang Budach*

Promatrana je adsorpcija pirena na različitim modelnim granicama faza kao što su zrak/voda, zrak/lipidni monosloj, živina elektroda/otopina i živina elektroda modificirana lipidnim slojevima. Uporabljene su spektroskopske (apsorpcijska, refleksna i fluorescentna spektroskopija), monoslojne (mjerenje površinskog tlaka  $\pi$  i površinskog potencijala  $\Delta V$ ) i elektrokemijske metode.

Svrha tih motrenja bila je procijeniti najvjerojatnije i najznačajnije procese koji utječu na raspodjelu i učinke vrlo hidrofobnih, odnosno gotovo netopivih organskih zagađivala u prirodnim vodenim sustavima.

Rezultati su pokazali da se molekule pirena ugrađuju u hidrofobnu jezgru lipidnih monoslojeva, mijenjajući transport mase i naboja kroz monoslojeve.